Catalysis Science & Technology c6cy02410f

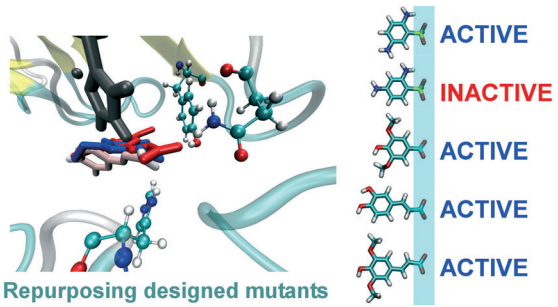

Q3

Repurposing designed mutants: a valuable strategy for computer-aided laccase engineering – the case of POXA1b

Valerio Guido Giacobelli, Emanuele Monza, M. Fatima Lucas, Cinzia Pezzella, Alessandra Piscitelli, Victor Guallar* and Giovanni Sannia*

The broad specificity of laccases, a direct consequence of their shallow binding site, makes this class of enzymes a suitable template to build specificity toward putative substrates.

Please check this proof carefully. **Our staff will not read it in detail after you have returned it.**

Translation errors between word-processor files and typesetting systems can occur so the whole proof needs to be read. Please pay particular attention to: tabulated material; equations; numerical data; figures and graphics; and references. If you have not already indicated the corresponding author(s) please mark their name(s) with an asterisk. Please e-mail a list of corrections or the PDF with electronic notes attached – do not change the text within the PDF file or send a revised manuscript. Corrections at this stage should be minor and not involve extensive changes. All corrections must be sent at the same time.

Please bear in mind that minor layout improvements, e.g. in line breaking, table widths and graphic placement, are routinely applied to the final version.

Please note that, in the typefaces we use, an italic vee looks like this: ν, and a Greek nu looks like this: ν.

We will publish articles on the web as soon as possible after receiving your corrections; **no late corrections will be made.**

Please return your **final** corrections, where possible within **48 hours** of receipt, by e-mail to: catalysis@rsc.org

Queries for the attention of the authors

Journal: **Catalysis Science & Technology**

Paper: **c6cy02410f**

Title: **Repurposing designed mutants: a valuable strategy for computer-aided laccase engineering – the case of POXA1b**

Editor's queries are marked on your proof like this Q1, Q2, etc. and for your convenience line numbers are indicated like this 5, 10, 15, ...

Please ensure that all queries are answered when returning your proof corrections so that publication of your article is not delayed.

Query Reference	Query	Remarks
Q1	For your information: You can cite this article before you receive notification of the page numbers by using the following format: (authors), Catal. Sci. Technol., (year), DOI: 10.1039/c6cy02410f.	
Q2	Please carefully check the spelling of all author names. This is important for the correct indexing and future citation of your article. No late corrections can be made.	
Q3	Please check that the inserted Graphical Abstract text is suitable. Please ensure that the text fits between the two horizontal lines.	
Q4	The meaning of the sentence beginning "The laccase peak..." is not clear - please provide alternative text.	
Q5	Ref. 1, 25 and 34: Please provide the page (or article) number(s).	
Q6	Ref. 1: Please provide the initial(s) for the 1st author.	

Catalysis Science & Technology

PAPER

Repurposing designed mutants: a valuable strategy for computer-aided laccase engineering – the case of POXA1b†

Cite this: DOI: 10.1039/c6cy02410f

Valerio Guido Giacobelli,‡[a] Emanuele Monza,‡[b] M. Fatima Lucas,[b] Cinzia Pezzella,[a] Alessandra Piscitelli,[a] Victor Guallar*[bc] and Giovanni Sannia*[a]

Received 17th November 2016,
Accepted 3rd January 2017

DOI: 10.1039/c6cy02410f

www.rsc.org/catalysis

The broad specificity of laccases, a direct consequence of their shallow binding site, makes this class of enzymes a suitable template to build specificity toward putative substrates. In this work, a computational methodology that accumulates beneficial interactions between the enzyme and the substrate in productive conformations is applied to oxidize 2,4-diamino-benzenesulfonic acid with POXA1b laccase. Although the experimental validation of two designed variants yielded negative results, most likely due to the hard oxidizability of the target substrate, molecular simulations suggest that a novel polar binding scaffold was designed to anchor negatively charged groups. Consequently, the oxidation of three such molecules, selected as representative of different classes of substances with different industrial applications, significantly improved. According to molecular simulations, the reason behind such an improvement lies in the more productive enzyme–substrate binding achieved thanks to the designed polar scaffold. In the future, mutant repurposing toward other substrates could be first carried out computationally, as done here, testing molecules that share some similarity with the initial target. In this way, repurposing would not be a mere safety net (as it is in the laboratory and as it was here) but rather a powerful approach to transform laccases into more efficient multitasking enzymes.

Introduction

Fungal laccases (benzenediol: oxygen oxidoreductase, EC 1.10.3.2) are among the best known and greenest biocatalysts in biotechnology.[1] The active core of this class of enzymes consists of four copper ions arranged in two clusters: the T1 copper, placed in the proximity of the protein surface, and the T2/T3 trinuclear cluster (TNC), buried in the protein interior. Substrate oxidation takes place at the T1 site, where H456 and D205 (POXA1b numbering) are the first electron and proton acceptors (if proton transfer is needed).[2] Then, the electron is transferred to the TNC, where oxygen reduction occurs.[3] Laccases have a high potential impact in several biotechnological areas, including pulp and paper, food, furniture manufacturing, and biofuels or nano-biodevices (biosensors and biofuel cells). Furthermore, the use of fungal laccases and/or laccase mediator systems (LMS) for organic synthesis has been studied in depth, ranging from the production of pharmacological compounds (*e.g.* antibiotics, antitumor and antiviral agents) to that of complex polymers.[1,4–6] Such a broad range of applications has led to numerous engineering efforts,[7] including computer-aided strategies,[8,9] aiming at enhancing their activity and/or stability for industrial application. As for specificity, laccases are very promiscuous enzymes, most likely as a consequence of a superficial, shallow binding site which cannot guarantee the optimal positioning for ET for all the putative substrates. Consequently, the T1 pocket could be modified *tout court* to lock the desired substrate in a highly reactive conformation, anchoring it to polar groups. Computational techniques are very promising

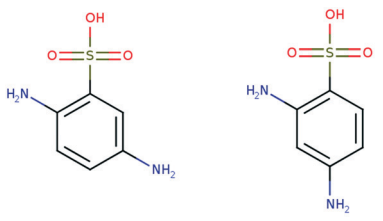

2,5-dabsa 2,4-dabsa

Scheme 1 Chemical structures of 2,5- and 2,4-dabsa.

[a] *Department of Chemical Sciences, University of Naples Federico II, Via Cintia 4, 80126 Naples, Italy. E-mail: sannia@unina.it*
[b] *Joint BSC-CRG-IRB Research Program in Computational Biology, Barcelona Supercomputing Center, c/Jordi Girona 29, 08034 Barcelona, Spain. E-mail: victor.guallar@bsc.es*
[c] *Institució Catalana de Recerca i Estudis Avançats (ICREA), Passeig Lluís Companys 23, 08010 Barcelona, Spain*

† Electronic supplementary information (ESI) available. See DOI: 10.1039/c6cy02410f

‡ These authors contributed equally to this work.

as they provide an atomistic mapping of both substrate binding and oxidation.[8–10]

In this work, a computational evolution protocol is applied to render the oxidation of 2,4-diamino-benzenesulfonic acid (2,4-dabsa) by POXA1b, a fungal (*Pleurotus ostreatus*) laccase with an unusually high stability at alkaline pH,[11] possible. The substrate of interest, 2,4-dabsa, is a dye precursor just like its constitutional isomer, 2,5-dabsa (Scheme 1). Although 2,4-dabsa is significantly cheaper than 2,5-dabsa, the latter is readily oxidized by POXA1b at alkaline pH and 60 °C while the former is not. Therefore, there is interest in redesigning POXA1b to oxidize 2,4-dabsa, aiming to lower the cost of dye production. Although the engineering effort did not produce an improved variant toward the oxidation of 2,4-dabsa, the mutant variants display a significantly increased ability to oxidize three typical substrates of laccases. Molecular calculations suggest that such an improvement is the consequence of specific enzyme–substrate interactions accumulated during computational evolution. The consequences for computer-aided laccase engineering and mutant repurposing are discussed.

Experimental section

Homology modeling and system setup

The POXA1b structure was generated through Prime homology modeling,[12,13] automatically selecting 1GYC.pdb (60% sequence identity) as a template. POXA1b is characterized by a longer C-terminal tail, which could be placed outside (**1**) or inside (**2**) the oxygen cavity (Fig. 1). The structure of **2** was taken from a previous work.[14] The POXA1b structures (**1** and **2**) were prepared with Protein Preparation Wizard.[15] The protonation states of titratable residues were generated with PROPKA[16] and double-checked with the H++ server,[17] simulating pH 8.

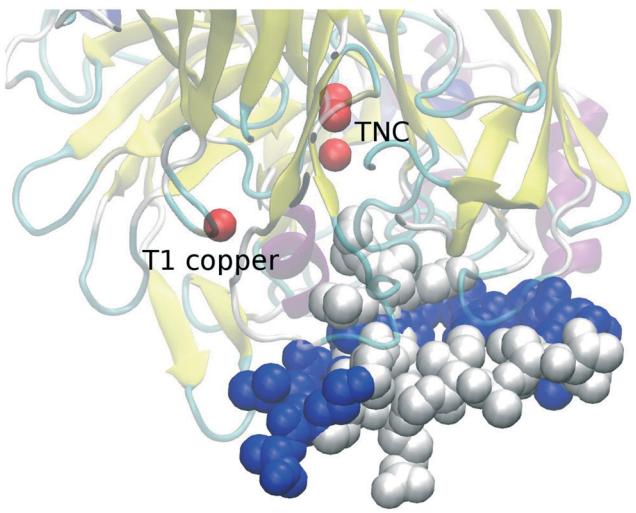

Fig. 1 Conformations of **1** (blue VDW spheres) and **2** (white VDW spheres) obtained from homology modeling.

Molecular dynamics

Molecular dynamics (MD) simulations were performed with GROMACS[18] for **1** and **2** to refine the initial homologous structures. The enzymes were solvated with a 10 Å layer of water molecules in a dodecahedral box, adding enough ions for neutralization and a 0.15 M NaCl buffer. The systems prepared were equilibrated as follows: i) solvent minimization; ii) system minimization; iii) 200 ps system warm up from 15 to 298 K at constant volume; iv) 200 ps at constant volume and 298 K; and v) 200 ps at 298 K and 1 bar. Then, a 200 ns production run was performed at 298 K and 1 bar for each model. The AMBER99 force-field[19] and the SPC explicit water model[20] were used. The copper ions, modeled in their reduced (+1) state (to attenuate charge repulsion in the TNC), the coordinating atoms and their nearest neighbours were restrained to their initial positions with stiff 10 000 kJ mol^{-1} nm^{-2} harmonic constraints. The temperature was regulated with velocity rescaling[21] with a relaxation time of 0.1 ps, and the pressure was controlled with a Parrinello-Rahman barostat[22] with isotropic coupling and a relaxation time of 2.0 ps. The LINCS algorithm[23] was employed to constrain all bond lengths, allowing a time step of 2.0 fs. A 10 Å cutoff was used for non-bonded interactions together with the particle mesh Ewald method.[24] It is well known that homology models can fall apart when subjected to MD,[25] thus a 1000 kJ mol^{-1} nm^{-2} harmonic constraint was applied to the secondary structure elements (helices and sheets) for the first 40 ns and lowered to 10 kJ mol^{-1} nm^{-2} for the rest of the simulation.

PELE sampling

The laccase–substrate conformational space, for the wild type (wt) and mutant variants and for all the substrates mentioned in the text, was sampled with PELE,[26,27] our in-house software. The substrate, initially placed in front of the T1 cavity, was randomly translated and rotated within 15 Å of the T1 copper. The laccase was perturbed according to an anisotropic network model (ANM) applied to all the alpha carbons in the system. Residues within 10 Å of the substrate were minimized after both the substrate and the enzyme were perturbed. Throughout the study, (PELE) binding energies refer to protein–substrate interaction potential energies.

PELE design

The initial conformation for the design was selected from the wt PELE sampling among the structures that exhibit catalytic contacts with H456 and D205, the first electron and proton acceptor, respectively. Then, every residue within 10 Å of the substrate was mutated to all of the possible remaining 19 amino acids; mutated residues included: T160, G161, V162, P163, H164, C204, S206, N207, A239, N263, S264, F331, P333, A336, A391, G392, P393, P395, W455, P510, and L511. The ligand was perturbed with very small translations and rotations while the protein backbone was subjected to small ANM displacements. Every residue within 10 Å of the

substrate was energy minimized. The simulation of each mutant (and the wild type) lasted 1 hour, accumulating ~30 Monte Carlo steps (~20 accepted). The enzyme–substrate interaction energy was used to score each mutant, while keeping an eye on the substrate's solvent accessible surface area (SASA). An example of input file for both PELE sampling and design is available in the ESI† and can be uploaded to the PELE server[28] to reproduce the results in this paper.

Treatment of substrate and metal centers in PELE

The substrates' geometries were optimized at the M06/6-31G* level of theory, modeling the solvent with the Poisson–Boltzmann model, using Jaguar.[29] The atomic ESP charges were calculated from the optimized structure and used for PELE. The OPLS parameters were assigned to the ligand with Schrödinger's hetgrp_ffgen utility and a rotamer library was generated with the in-house PELE's scripts using Macromodel.[30] The copper ions and their coordination atoms plus their nearest neighbors were constrained during PELE sampling with 200 kcal mol^{-1} $Å^{-2}$ harmonic constraints on their atomic positions.

Materials

ABTS (2,2′-azino-bis(3-ethylbenzothiazoline-6-sulfonic acid) diammonium salt), 2,4-dabsa, sinapic acid, syringic acid, and caffeic acid were purchased from Sigma-Aldrich. All chemicals were of reagent-grade purity. Expression vectors and yeast strains were purchased from Biogrammatics, Ltd (Las Palmas Dr, Carlsbad, CA, USA).

Construction and screening of POXA1b expressing mutants

The QuikChange site-directed mutagenesis kit was purchased from Agilent Technologies. Synthetic oligonucleotides were produced by Eurofins Genomics. Plasmid purification kits were purchased from Qiagen, Inc. A synthetic gene encoding for *Pleurotus ostreatus* POXA1b was designed and optimized according to *P. pastoris* codon usage. The gene product was restricted with BsaI and ligated to the corresponding site of the pJGG_αkR vector in-frame with the α-factor (signal peptide) under the control of the constitutive GAP promoter, yielding the recombinant plasmid pJGGαKR_POXA1b. Mutagenesis of the wild type POXA1b cDNA within the plasmid pJGGαKR_POXA1b was performed by following the instructions provided in the QuikChange site-directed mutagenesis kit. The sense oligonucleotides used for mutagenesis are as follows:

5′ CCTTGTCTTTGACTGGTGTTCCACACCCAGACTCCAC 3′ for Val162Ser,

5′ CCTTGTCTTTGACTGGTGTTCCACACCCAGACTCCAC 3′ for Val162His,

5′ CTTGAACTTCGCTTTCGACCCTGCTACTGC 3′ for Phe331Tyr, and

5′ CGCTTACGACCCTGCTACTGCTTTGTTCACTGCTAACAACC 3′ for Ala336Asn.

The complementary antisense oligonucleotides also necessary for the mutagenesis are not shown. The mutagenized recombinant plasmids (pJGGαKR_V162S_F331Y_A336N and pJGGαKR_V162H_F331Y_A336N) were then used to transform ultracompetent cells as described by the manufacturer. Recombinant plasmids were purified from 5 mL overnight cultures using the Qiagen miniprep system. The presence of the correct mutation was confirmed in all constructs by DNA sequencing (Eurofins Genomics). The mutagenized plasmids were linearized by *BsiWI* and transformed into *P. pastoris* BG-10 by electroporation.[31] The cell suspension was spread on YPDS (10 g l^{-1} yeast extract; 20 g l^{-1} bacto tryptone; 20 g l^{-1} glucose; 182.2 g l^{-1} sorbitol) plates containing 900 μg ml^{-1} G418 and incubated for 3–7 days at 28 °C until colony formation. The colonies were collected, inoculated in Minimal Dextrose medium (MD) (13 g l^{-1} yeast nitrogen base with ammonium sulfate w/o amino acids, 4×10^{-4} g l^{-1} biotin, 20 g l^{-1} glucose), and grown at 28 °C on a rotary shaker (250 rpm). The colonies were then streaked on solid MD medium containing the laccase chromogenic substrate ABTS (13 g l^{-1} yeast nitrogen base with ammonium sulfate w/o amino acids; 4×10^{-4} g l^{-1} biotin; 20 g l^{-1} glucose, 0.6 mM $CuSO_4$ and 0.2 mM ABTS) to verify the expression of the recombinant proteins as well as on YPDS (10 g l^{-1} yeast extract; 20 g l^{-1} bacto tryptone; 20 g l^{-1} glucose; 182.2 g l^{-1} sorbitol) with 900 μg ml^{-1} G418. Recombinant pJGGαKR_V162S_F331Y_A336N and pJGGαKR_V162H_F331Y_A336N cultures selected from solid screening assay were inoculated in 20 ml BMMY (13 g l^{-1} yeast nitrogen base with ammonium sulfate without amino acids; 10 g l^{-1} yeast extract; 20 g l^{-1} peptone; 100 mM potassium phosphate, pH 6.0; 4×10^{-4} g l^{-1} biotin; 0.5% methanol) medium in a 100 ml shake flask. These cultures were grown for 8 days at 28 °C on a rotary shaker (250 rpm).

Assay of laccase activity

Culture aliquots were collected daily and assayed for cell density and extracellular laccase activity. Laccase activity in the culture supernatant was assayed at room temperature, monitoring the oxidation of ABTS at 420 nm ($\varepsilon_{420} = 3.6 \times 10^4$ M^{-1} cm^{-1}): the assay mixture contained 2 mM ABTS and 0.1 M Na-citrate buffer, pH 3.0. Purified laccase activity towards 2,4-dabsa was assayed at 60 °C temperature, monitoring the oxidation of 2,4-dabsa in the visible spectrum. The mixture contained 25 mM 2,4-dabsa and 0.1 M Tris–HCl buffer, pH 8.0.

Production and purification of POXA1b and mutated laccases

Recombinant *P. pastoris* cells expressing the two POXA1b mutants were inoculated in 50 ml BMMY medium in a 250 ml baffled shake flask. These precultures were grown for one day at 28 °C on a rotary shaker (250 rpm), then a volume of the suspension sufficient to reach a final OD600 value of 1.0 was used to inoculate 1 liter shake flasks containing 250 ml of BMMY medium. Cells were grown on a rotary shaker (250 rpm) at 28 °C and 3.75 ml of methanol was added to the

culture each day of growth to induce protein expression. The cultures were concentrated to 20 ml in a Pall multi-cassette system (10 kDa cutoff membrane). The samples were applied to an anion-exchange column (Hi-Prep 16/10) equilibrated with 20 mM Tris–HCl (pH 8.0) at a flow rate of 0.7 ml min^{-1}. The retained proteins were eluted with a gradient of 20 mM Tris–HCl (pH 8.0) plus 1 M NaCl. The laccase peaks were pooled, concentrated and dialysed against 20 mM Tris–HCl (pH 8.0). The active fractions were brought to 100% ammonium sulfate saturation and then centrifuged at 9300*g* for 10 min. The precipitated proteins were dissolved in 20 mM Tris–HCl (pH 8.0) and dialysed against the same buffer. A volume of 5 ml of dialyzed protein solution was transferred to a HiLoad 16/600 Superdex 200 pg column, equilibrated with 20 mM Tris–HCl (pH 8.0) plus 0.2 M NaCl, and eluted using the same buffer at a flow rate of 0.5 ml min^{-1}. Fractions were collected and dialysed against 20 mM Tris–HCl (pH 8.0). The dialysed samples were assayed for laccase activity and protein concentration. The specific activities of both purified enzyme variants were comparable to that of the wild-type.

Biochemical characterization of laccase variants

The oxidation of substrates by the purified laccase was determined spectrophotometrically (UVIKON 930, Kontron Instruments) at the specific wavelength of each substrate. The assays were performed by measuring the increase in the Abs 470 nm for syringic acid (ε = 0.5 mM^{-1} cm^{-1}), Abs 470 nm for caffeic acid (ε = 1.8 mM^{-1} cm^{-1}) and Abs 595 nm for sinapic acid (ε = 0.3 mM^{-1} cm^{-1}). The molar extinction coefficients of the three fully oxidized substrates were determined from their corresponding calibration curves. The kinetic constants K_M and V_{max} of the enzymes were determined using a Michaelis–Menten plot with syringic and caffeic acids. The kinetic constants K_i, K_M and V_{max} of the enzymes were determined in the case of sinapic acid using the equation reported below.[32] All substrates were dissolved in 20 mM Tris–HCl (pH 8.0).

$$V = \frac{V_{max}[S]}{K_M + [S] + [S]^2/K_I} \quad (1)$$

Results and discussion

Refinement of POXA1b models

The presence of a protruding C-terminal tail, compared to other laccases from basidiomycetes, has been previously observed in POXA1b.[33] According to homology modeling, such a tail could be placed either outside (**1**) or inside (**2**) the oxygen cavity (Fig. 1). MD simulations were performed to refine the models and establish whether **1** or **2** (or none of them) is the best representation of the system. Simulation of **1** converged in ~50 ns (Fig. 2, simulation stopped at ~160 ns), keeping the C-terminal away from the oxygen cavity (Fig. 3). In contrast, **2** is rather unstable (Fig. 2), resulting in the escape of the C-terminal from the protein interior, roughly matching **1** (Fig. 2). It follows that, according to the simulation, the C-terminal is more stable on the protein surface than in the interior. Moreover, the C-terminal of **1** directly interacts with the active site, adding a further degree of complexity to the design. Such a finding makes POXA1b's

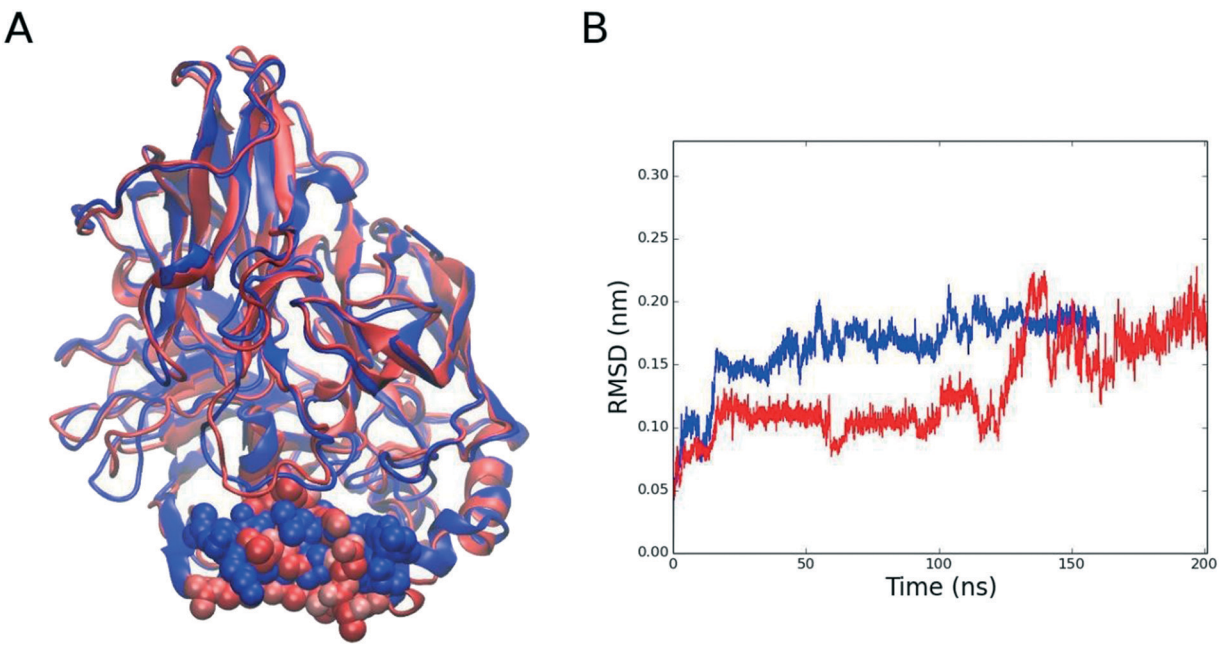

Fig. 2 A) Final snapshot from the MD simulation of **1** (blue) and **2** (red). The C-terminal tail is represented by VDW spheres. B) Heavy atom RMSD plots from the MD simulations of **1** (blue) and **2** (red).

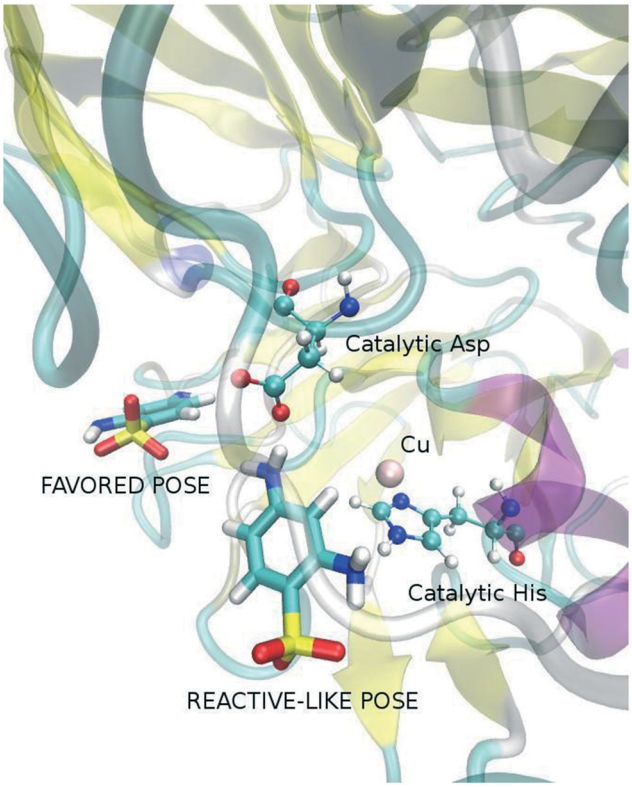

Fig. 3 Favored (best binding) and reactive-like (catalytic contacts) poses from PELE sampling for 2,4-dabsa.

C-terminal somewhat different with respect to that observed for *Melanocarpus albomyces* laccase, which is also resistant at alkaline pH. Its C-terminus is located in the proximity of the oxygen channel, obstructing small molecules' passage.[34] Nonetheless, the characterization of the truncated POXA1b mutants highlighted the key role of the C-terminus tail in protein stability at alkaline pH.[33]

Computational comparison of 2,4- *vs.* 2,5-dabsa

Binding of 2,4- and 2,5-dabsa in the T1 pocket was simulated with 96 independent 48 hour PELE runs. Inspection of the structures within 5 kcal mol^{-1} of the lowest PELE binding energy value (within 12 Å) reveals that no catalytic contact (*i.e.* H-bonds with H456 and D205, Scheme 2) is engaged with 2,4-dabsa (Fig. 3). In order to find a pose that displays catalytic interactions, it is necessary to climb the PELE binding energy ladder by ~30 kcal mol^{-1} (Fig. S3;† note that this value is a protein–ligand interaction energy, not a proper binding energy). Such an energy difference poses a great obstacle to oxidation, since the enzyme severely selects unproductive poses, *i.e.* with non-optimal electron tunnelling between the substrate and the T1 copper, slowing 2,4-dabsa oxidation down. The same analysis revealed that 2,5-dabsa displays such catalytic contacts with H456 in 13% of the low-lying binding energy conformations (Fig. S4†), but never with D205. Therefore, based on enzyme–substrate sampling, 2,4-dabsa binds unproductively to the T1 site compared to 2,5-dabsa; such a distinct binding preference might be ascribed to the different orientations of the amino groups in the benzene ring, which determines diverse H-bonding patterns with the enzyme.

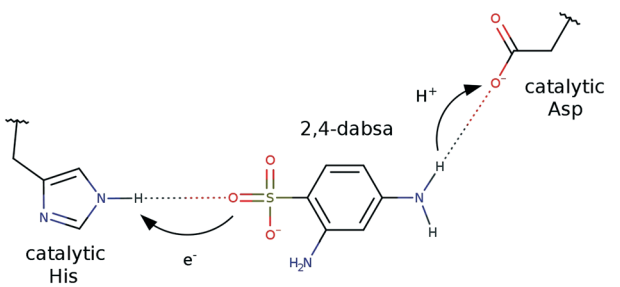

Scheme 2 Expected catalytic contacts.

A further cause for the different reactivities of the two isomers might lie in their different propensities for oxidation. This possibility was addressed by comparing the energy of the HOMO orbitals of 2,4- and 2,5-dabsa. According to Koopmans' theorem, the negative of the HOMO energy of a molecule corresponds to its ionization energy,[35] assuming no subsequent orbital relaxation (and neglecting electronic correlation). The geometry optimization of both isomers at the RHF/6-31G* level predicts the ionization energy of 2,4-dabsa to be larger by ~175 meV. Thus, not only does 2,4-dabsa have a worse interaction with the enzyme but it is also harder to oxidize than 2,5-dabsa.

Based on the above enzyme–substrate analysis, and following recent studies indicating the importance of the substrate binding event in laccases,[8–10] the engineering efforts were focused on the formation of (in principle) more reactive conformations of the Michaelis complex. Such a classical study does not require quantum chemical calculations, while tuning 2,4-dabsa oxidability inside the T1 pocket would.[8] Moreover, the outcome of this engineering effort would be a better starting point to target the oxidability of 2,4-dabsa. Finally, increasing the redox potential of the T1 copper is not straightforward and it does not guarantee success.[36–39] Therefore, the reactive-like pose depicted in Fig. 3 was selected as the initial template for the design, aiming at improving the enzyme–substrate interaction energy of such a binding mode, hence its statistical importance in the active site.

Design of a more reactive Michaelis complex

An evolutionary strategy was employed to accumulate beneficial mutations at each computational mutagenesis round (Fig. 4). During an evolution round, a mutation was considered beneficial if the binding energy improved by 5 kcal mol^{-1} or more; then, one candidate was selected and used as the starting template for the next round. It should be noted that, at each of these rounds, the mutants showing improved PELE binding energy were all visually inspected, bringing

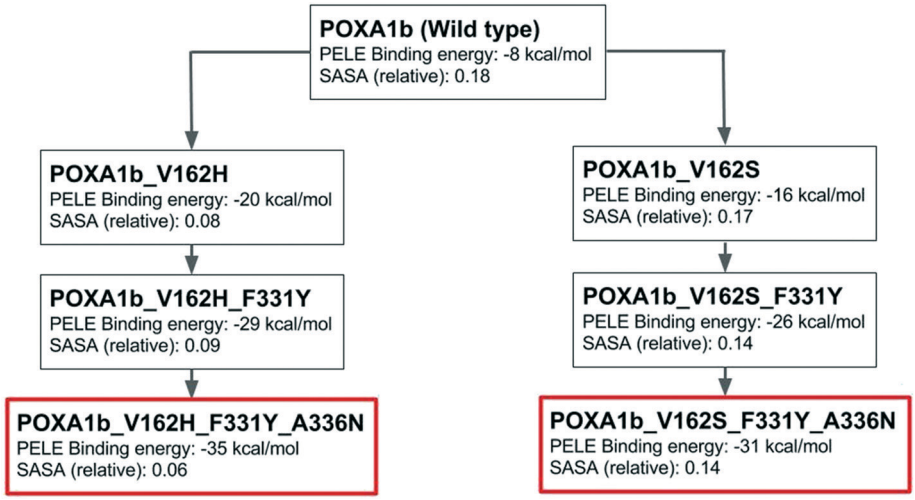

Fig. 4 Evolutionary strategy and results of POXA1b design toward 2,4-dabsa oxidation.

chemical intuition into play. In the first round, two mutations looked promising due to a great increase in PELE's binding energy and, in one case, a significant drop in SASA (hence a possible decrease in reorganization energy[40]): V162H and V162S (Fig. 4).

Although other mutations present interesting values (Table S1†), they were discarded in favor of V162H and V162S for one of the following reasons: i) they involved Gly/Pro (as the starting amino acid), which might trigger important loop conformational changes due to their flexibility/rigidity which cannot be captured at this level of sampling (they would need extensive sampling to confirm their reliability); ii) unless they introduce outstanding improvement, positive charges are avoided as they might inhibit oxidation; iii) they were located on the C-terminal tail, whose conformation is the most fragile aspect of the model; and iv) visual inspection suggested caution.

After the first round, computational evolution was branched, further designing both the V162H and V162S variants (Fig. 4). In the second round of both V162H and V162S branches, F331Y was chosen, while in round 3, A335N was selected for both branches as well. Computational evolution was stopped at this point.

In both branches, three new H-bonds with the sulfonate group of 2,4-dabsa were introduced (Fig. 5), increasing the binding energy by more than 20 kcal mol^{-1} (SASA is also significantly reduced in the V162H branch). Therefore, the evolved active sites should be able to select the substrate in a reactive conformation with much higher frequency. In order to test this hypothesis, a new PELE extensive sampling run was carried out for the evolved triple mutants, as previously done for the POXA1b wt; the catalytic and designed contacts were then checked in the structures within 5 kcal mol^{-1} of the lowest binding energy value. Nicely, for the V162S branch, all the designed H-bonds and the H456–sulfonate contact were retained in all the binding modes, while the D205–amino contact was formed in 40% of the cases. In contrast, this last contact is never formed in the V162H branch. On top of that, although H456 and N336 interact with the sulfonic group, the other designed contacts did not form as planned: the side chains of Y331 and H162 interact with the amino groups instead (Fig. S1†). Still, the resulting binding

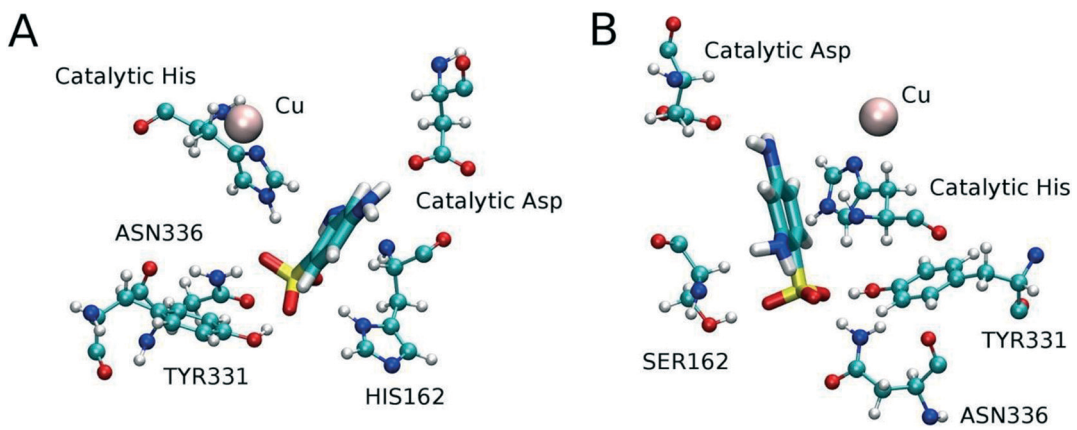

Fig. 5 Structural model of the designed triple mutants. A) V162H branch; B) V162S branch.

mode is more reactive than in POXA1b (Fig. 3): an efficient through bond (sulfonate–H456) electron tunnelling path is set, while the aminic proton could be abstracted by a water molecule (if proton transfer occurs simultaneously), although it is not the optimal path. Therefore, it was decided to test also the V162H branch triple mutant in the lab.

Experimental validation, rationalization of results and mutant repurposing

Regardless of the promising mutant validation with PELE sampling, the evolved variants were inactive towards 2,4-dabsa, just as POXA1b. The possible reasons behind this unsatisfying result are as follows: i) the homology model is inaccurate in the active site description due to the presence of the C-terminal and ii) 2,4-dabsa is not significantly oxidized by the T1 copper (*i.e.* the ET driving force is positive and too large). While the first point is difficult to verify, the ~175 mV difference in ionization energy between the dabsa isomers suggests that it might be a substrate oxidability issue. Further analysis of these possibilities was studied by testing additional ligands.

Although the designed variants failed to oxidize the target substrate, their putative ability to lock in place 2,4-dabsa's sulfonic group could be exploited to improve the oxidation of other negatively charged substrates. As reported in the literature,[10] the introduction of polar amino acids in the T1 pocket enhances its binding interaction with sinapic acid, a negatively charged substrate (Scheme 3). Since the presented computational evolution effort yielded a more polar T1 site, the oxidation of sinapic acid was characterized with experimental methods, aiming at verifying if the mutant variants can oxidize it better. In addition, caffeic and syringic acids (Scheme 3) were also selected for laboratory characterization in terms of their chemical similarity to sinapic acid. These two molecules are representative of two different classes of substances, hydroxycinnamates and trihydroxybenzoic acid, with different industrial applications.[41,42] By testing and simulating these substrates, which are regularly oxidized by laccases, it is possible to assess if the designed binding moiety is effective and leads to activity improvement.

As can be seen in Tables 1–3, the efficiency constant (k_{cat}/K_M) of the triple mutants is higher than that of POXA1b for all the substrates (Tables 1–3). Interestingly, sinapic acid substrate inhibition is also attenuated in the evolved variants, as reflected by the larger inhibition constant (K_i) values, while an overall tendency of increasing K_M and k_{cat} can be observed (Table 3). Since the kinetic data for this substrate are obtained from a substrate inhibition model (the substrate binds unproductively to the enzyme while hindering the formation of productive enzyme–substrate adducts[32]), the trend of the kinetic constants implies that either the unproductive poses are destabilized or the productive conformations are stabilized in the mutant. The second hypothesis could be true despite the larger K_M values, since this constant would increase with k_{cat} in a steady-state kinetic regime.[43]

In order to obtain a molecular mechanism for the increase in substrate oxidation, the binding of these three substrates in the T1 pocket of POXA1b and its evolved variants was simulated with PELE. The objective was to verify whether such improved catalytic performance is related to the larger population of conformations in which the carboxyl group (which is deprotonated at pH 8) is H-bonded to H456. As a matter of fact, POXA1b never shows H-bonds between H456 and the substrates, forcing an inefficient through-space electron tunnelling between the substrate and the T1 center. On the other hand, H-bonds between the substrate and H456 have a significant population for every mutant–substrate pair, which ranges from 29 to 81% (Tables 1–3) among the structures within 5 kcal mol^{-1} of the binding energy minima and within 10 Å of the T1 copper. This contact facilitates a through-bond electron tunnelling, which greatly improves electron transfer. Remarkably, the sinapic acid–V162S branch mutant pair, the one that experiences the largest improvement in k_{cat} (~15 fold, Table 3), exhibits the largest population of this contact (81%) and forms all the designed H-bonds in 61% of the cases (Fig. 6). Finally, it is worth noting that no contact is formed between the substrate and D205 in any variant–substrate pair, meaning that such a contact is not indispensable (water molecules can assist deprotonation), although design toward the instauration of such interaction could further improve oxidation (especially due to the farther vicinity of a negative charge that could shift up the HOMO energy of the substrates).

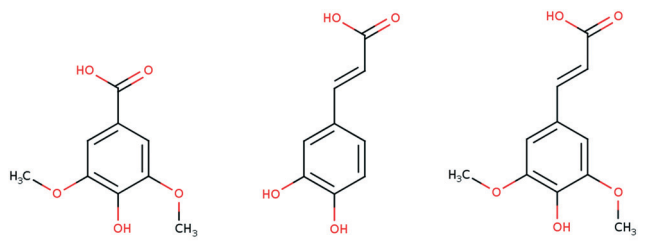

Scheme 3 Chemical structures of syringic, caffeic and sinapic acids.

Consequences for laccase design

Although the initial design was not successful, the repurposing effort suggests (both in its experimental and computational validation) that the non-specific reaction site of laccases can be a valuable template to build more specific interactions with a target substrate. This can be implemented with the presented computational methodology, increasing the affinity of the substrate for the enzyme in a highly reactive conformation. Nonetheless, laccase design proved to be a delicate multidimensional problem which requires to always take an electron transfer driving force into account. As seen, if a target substrate is poorly oxidizable, the electron transfer driving force might become a crucial design parameter, tunable as shown recently.[9]

Table 1 Experimental kinetic constants and population of structures exhibiting catalytic carboxyl-H456 H-bonds during PELE sampling for the oxidation of caffeic acid by POXA1b and the designed triple mutants

	K_M (mM)	k_{cat} (s^{-1})	k_{cat}/K_M (mM^{-1} s^{-1})	Sub–H456 H-bonds (%)
POXA1b	3.52 ± 0.53	1262 ± 60	360 ± 60	0
V162H branch	0.47 ± 0.11	1122 ± 54	2805 ± 54	50
V162S branch	3.65 ± 0.57	4184 ± 35	1162 ± 35	29

Table 2 Experimental kinetic constants and population of structures exhibiting catalytic carboxyl-H456 H-bonds during PELE sampling for the oxidation of syringic acid by POXA1b and the designed triple mutants

	K_M (mM)	k_{cat} (s^{-1})	k_{cat}/K_M (mM^{-1} s^{-1})	Sub–H456 H-bonds (%)
POXA1b	1.22 ± 0.11	1775 ± 87	1400 ± 87	0
V162H branch	1.35 ± 0.27	2700 ± 54	2000 ± 54	60
V162S branch	0.82 ± 0.25	6997 ± 87	8000 ± 87	50

Table 3 Experimental kinetic constants and population of structures exhibiting catalytic carboxyl-H456 H-bonds during PELE sampling for sinapic acid by POXA1b and the designed triple mutants

	K_M (mM)	k_{cat} (s^{-1})	k_{cat}/K_M (mM^{-1} s^{-1})	K_i (mM)	Sub–H456 H-bonds (%)
POXA1b	0.13 ± 0.05	6681 ± 100	51 392 ± 100	1.23 ± 0.09	0
V162H branch	0.41 ± 0.03	39 113 ± 500	95 397 ± 500	2.44 ± 0.09	66
V162S branch	0.67 ± 0.02	97 126 ± 600	144 964 ± 600	1.49 ± 0.08	81

Repurposing should not be a mere safety net (as it was in this case) but rather an effective strategy for industrial enzyme production. Computational design toward a given substrate could be accompanied on-the-fly by the *in silico* evaluation of a database of putative substrates, possibly selecting a subset based on target molecular similarity. In this way, several processes could be improved at the cost of one or a new design line for a particularly promising substrate could be opened. Ideally, variant search should not be fossilized on a fixed laccase either. These enzymes present great diversity in their T1 pockets that could be exploited to design the best host as much as possible for a (class of) substrate(s). Even if a very promising laccase did not function under the desired working conditions (pH, temperature, presence of ions and/or co-solutes, *etc.*), the enzyme could be designed to adapt to them. Therefore, a future where several laccases are computationally evolved against many substrates can be envisioned. Pushing further, efficient chimeric laccases might be designed by conveniently stitching portions of proteins from different laccases with computational techniques.[44]

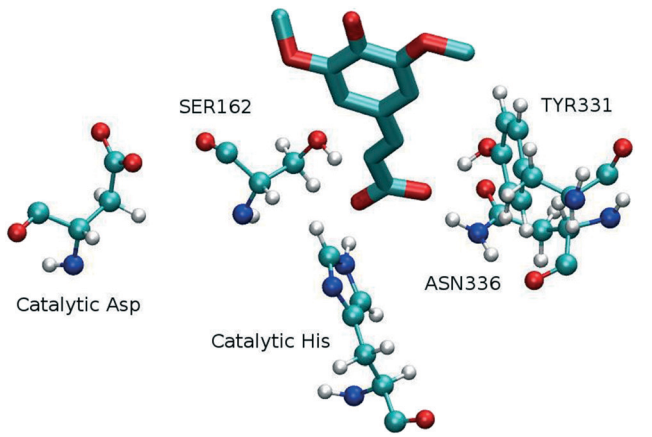

Fig. 6 PELE sampling result for the binding of sinapic acid in the active site of the V162S branch triple mutant.

Conclusions

This work showed that the T1 site is a promiscuous template to increase activity toward specific target substrates, through the design of stabilizing enzyme–substrate interactions in a highly reactive conformation. The experimental and computational validation of mutant repurposing suggests that this task could be achieved with the computational protocol proposed in this work. Nonetheless, it should be borne in mind that laccase design is an intricate multidimensional problem in which the ET driving force is an important factor. Likely due to the superficial and shallow nature of the T1 site, repurposing designed mutants to oxidize molecules that share some degree of similarity with the target proved to be effective. In the future, repurposing might be carried out computationally and subsequently validated experimentally, transforming laccases into more efficient multitasking enzymes.

Acknowledgements

This work was funded by INDOX (KBBE-2013-7-613549) European project and CTQ2013-48287-R Spanish National Project. V. G. and E. M. acknowledge Università degli Studi di Napoli

and Generalitat de Catalunya for their respective predoctoral fellowships.

References

Q6 Q5 1 Shraddha, R. Shekher, S. Sehgal, M. Kamthania and A. Kumar, *Enzyme Res.*, 2011, **2011**.

2 T. Bertrand, C. Jolivalt, P. Briozzo, E. Caminade, N. Joly, C. Madzak and C. Mougin, *Biochemistry*, 2002, **41**, 7325–7333.

3 P. Giardina, V. Faraco, C. Pezzella, A. Piscitelli, S. Vanhulle and G. Sannia, *Cell. Mol. Life Sci.*, 2010, **67**, 369–385.

4 S. Riva, *Trends Biotechnol.*, 2006, **24**, 219–226.

5 A. Kunamneni, F. J. Plou, A. Ballesteros and M. Alcalde, *Recent Pat. Biotechnol.*, 2008, **2**, 10–24.

6 C. Pezzella, L. Guarino and A. Piscitelli, *Cell. Mol. Life Sci.*, 2015, **72**, 923–940.

7 I. Pardo and S. Camarero, *Cell. Mol. Life Sci.*, 2015, **72**, 897–910.

8 E. Monza, M. F. Lucas, S. Camarero, L. C. Alejaldre, A. T. Martínez and V. Guallar, *J. Phys. Chem. Lett.*, 2015, **6**, 1447–1453.

9 G. Santiago, F. de Salas, M. F. Lucas, E. Monza, S. Acebes, Á. T. Martinez, S. Camarero and V. Guallar, *ACS Catal.*, 2016, **6**, 5415–5423.

10 I. Pardo, G. Santiago, P. Gentili, F. Lucas, E. Monza, F. J. Medrano, C. Galli, A. T. Martínez, V. Guallar and S. Camarero, *Catal. Sci. Technol.*, 2016, **6**, 3900–3910.

11 P. Giardina, G. Palmieri, A. Scaloni, B. Fontanella, V. Faraco, G. Cennamo and G. Sannia, *Biochem. J.*, 1999, **341**, 655.

12 M. P. Jacobson, D. L. Pincus, C. S. Rapp, T. J. F. Day, B. Honig, D. E. Shaw and R. A. Friesner, *Proteins*, 2004, **55**, 351–367.

13 M. P. Jacobson, R. A. Friesner, X. Zhexin and H. Barry, *J. Mol. Biol.*, 2002, **320**, 597–608.

14 G. Festa, F. Autore, F. Fraternali, P. Giardina and G. Sannia, *Proteins*, 2008, **72**, 25–34.

15 G. M. Sastry, M. Adzhigirey, T. Day, R. Annabhimoju and W. Sherman, *J. Comput.-Aided Mol. Des.*, 2013, **27**, 221–234.

16 M. H. M. Olsson, C. R. Søndergaard, M. Rostkowski and J. H. Jensen, *J. Chem. Theory Comput.*, 2011, **7**, 525–537.

17 J. C. Gordon, J. B. Myers, T. Folta, V. Shoja, L. S. Heath and A. Onufriev, *Nucleic Acids Res.*, 2005, **33**, W368–W371.

18 S. Pronk, S. Páll, R. Schulz, P. Larsson, P. Bjelkmar, R. Apostolov, M. R. Shirts, J. C. Smith, P. M. Kasson, D. van der Spoel, B. Hess and E. Lindahl, *Bioinformatics*, 2013, **29**, 845–854.

19 Y. Duan, C. Wu, S. Chowdhury, M. C. Lee, G. Xiong, W. Zhang, R. Yang, P. Cieplak, R. Luo, T. Lee, J. Caldwell, J. Wang and P. Kollman, *J. Comput. Chem.*, 2003, **24**, 1999–2012.

20 K. Toukan, T. Kahled and R. Aneesur, *Phys. Rev. B: Condens. Matter Mater. Phys.*, 1985, **31**, 2643–2648.

21 G. Bussi, D. Donadio and M. Parrinello, *J. Chem. Phys.*, 2007, **126**, 014101.

22 M. Parrinello, *J. Appl. Phys.*, 1981, **52**, 7182.

23 B. Hess, H. Berk, B. Henk, H. J. C. Berendsen and G. E. Johannes, *J. Comput. Chem.*, 1997, **18**, 1463–1472.

24 U. Essmann, E. Ulrich, P. Lalith, M. L. Berkowitz, D. Tom, L. Hsing and L. G. Pedersen, *J. Chem. Phys.*, 1995, **103**, 8577.

25 A. Raval, R. Alpan, P. Stefano, M. P. Eastwood, R. O. Dror and D. E. Shaw, *Proteins: Struct., Funct., Bioinf.*, 2012.

26 K. W. Borrelli, A. Vitalis, R. Alcantara and V. Guallar, *J. Chem. Theory Comput.*, 2005, **1**, 1304–1311.

27 B. P. Cossins, A. Hosseini and V. Guallar, *J. Chem. Theory Comput.*, 2012, **8**, 959–965.

28 A. Madadkar-Sobhani and V. Guallar, *Nucleic Acids Res.*, 2013, **41**, W322–W328.

29 A. D. Bochevarov, H. Edward, T. F. Hughes, J. R. Greenwood, D. A. Braden, D. M. Philipp, R. David, M. D. Halls, Z. Jing and R. A. Friesner, *Int. J. Quantum Chem.*, 2013, **113**, 2110–2142.

30 F. Mohamadi, M. Fariborz, N. G. J. Richards, W. C. Guida, L. Rob, L. Mark, C. Craig, C. George, H. Thomas and W. Clark Still, *J. Comput. Chem.*, 1990, **11**, 440–467.

31 A. Piscitelli, A. Pennacchio, P. Cicatiello, J. Politi, L. De Stefano and P. Giardina, *Biosens. Bioelectron.*, 2016, **87**, 816–822.

32 T. D. H. Bugg, *Introduction to Enzyme and Coenzyme Chemistry*, 2012.

33 F. Autore, C. Del Vecchio, F. Fraternali, P. Giardina, G. Sannia and V. Faraco, *Enzyme Microb. Technol.*, 2009, **45**, 507–513.

34 N. Hakulinen, L.-L. Kiiskinen, K. Kruus, M. Saloheimo, A. Paananen, A. Koivula and J. Rouvinen, *Nat. Struct. Biol.*, 2002.

35 T. Koopmans, *Physica*, 1934, **1**, 104–113.

36 F. Xu, R. M. Berka, J. A. Wahleithner, B. A. Nelson, J. R. Shuster, S. H. Brown, A. E. Palmer and E. I. Solomon, *Biochem. J.*, 1998, **334**(Pt 1), 63–70.

37 F. Xu, A. E. Palmer, D. S. Yaver, R. M. Berka, G. A. Gambetta, S. H. Brown and E. I. Solomon, *J. Biol. Chem.*, 1999, **274**, 12372–12375.

38 P. Durão, I. Bento, A. T. Fernandes, E. P. Melo, P. F. Lindley and L. O. Martins, *J. Biol. Inorg. Chem.*, 2006, **11**, 514–526.

39 G. Macellaro, M. C. Baratto, A. Piscitelli, C. Pezzella, F. Fabrizi de Biani, A. Palmese, F. Piumi, E. Record, R. Basosi and G. Sannia, *Appl. Microbiol. Biotechnol.*, 2014, **98**, 4949–4961.

40 C. A. Bortolotti, M. E. Siwko, C. Elena, R. Antonio, S. Marco and C. Stefano, *J. Phys. Chem. Lett.*, 2011, **2**, 1761–1765.

41 V. Lettera, C. Pezzella, P. Cicatiello, A. Piscitelli, V. G. Giacobelli, E. Galano, A. Amoresano and G. Sannia, *Food Chem.*, 2016, **196**, 1272–1278.

42 P. Alvira, A. D. Moreno, D. Ibarra, F. Sáez and M. Ballesteros, *Biotechnol. Prog.*, 2013, **29**, 74–82.

43 P. W. Atkins and J. De Paula, *Atkins' Physical Chemistry*, 2002.

44 T. M. Jacobs, B. Williams, T. Williams, X. Xu, A. Eletsky, J. F. Federizon, T. Szyperski and B. Kuhlman, *Science*, 2016, **352**, 687–690.